# Accuracy of high-rate GPS for seismology

P. Elósegui,[1,2] J. L. Davis,[1] D. Oberlander,[3] R. Baena,[4] and G. Ekström[5]

Received 16 February 2006; revised 17 April 2006; accepted 3 May 2006; published 13 June 2006.

[1] We built a device for translating a GPS antenna on a positioning table to simulate the ground motions caused by an earthquake. The earthquake simulator is accurate to better than 0.1 mm in position, and provides the "ground truth" displacements for assessing the technique of high-rate GPS. We found that the root-mean-square error of the 1-Hz GPS position estimates over the 15-min duration of the simulated seismic event was 2.5 mm, with approximately 96% of the observations in error by less than 5 mm, and is independent of GPS antenna motion. The error spectrum of the GPS estimates is approximately flicker noise, with a 50% decorrelation time for the position error of ~1.6 s. We find that, for the particular event simulated, the spectrum of surface deformations exceeds the GPS error spectrum within a finite band. More studies are required to determine whether a generally optimal bandwidth exists for a target group of seismic events. **Citation:** Elósegui, P., J. L. Davis, D. Oberlander, R. Baena, and G. Ekström (2006), Accuracy of high-rate GPS for seismology, *Geophys. Res. Lett.*, *33*, L11308, doi:10.1029/2006GL026065.

## 1. Introduction

[2] "High-rate GPS" is a technique whereby positions are estimated at a rate of once per second or higher using the high-precision phase observations of the Global Positioning System (GPS). (In principle, this technique can be used with any global navigation satellite system (GNSS). However, so far, it has only been applied to GPS.) Developed only in the last few years, this technique has been used to determine the time-dependent surface displacements induced by the 2002 Denali earthquake [*Larson et al.*, 2003; *Bock et al.*, 2004], the 2003 San Simeon earthquake [*Ji et al.*, 2004], the 2003 Tokachi-Oki [*Miyazaki et al.*, 2004], the 2003 explosive activity of the Stromboli volcano [*Mattia et al.*, 2004], and the tsunami induced by the 2004 Kii peninsula earthquake [*Kato et al.*, 2005].

[3] Lack of independent measurements of the surface displacement limits an assessment of the accuracy of GPS in this new operating regime. The most obvious possibility is to compare to seismic measurements [e.g., *Larson et al.*, 2003; *Bock et al.*, 2004; *Miyazaki et al.*, 2004; *Ji et al.*, 2004], but seismometers potentially have a different accuracy spectrum than GPS and may have errors comparable to or, within some frequency bands, greater than those of GPS. This problem is exacerbated since seismic instruments record either velocity (seismometers) or acceleration (accelerometers), and thus require an integration (or double-integration) process for displacement, whereas GPS naturally produces position estimates.

[4] To this end, we have designed and constructed an "earthquake simulator" to enable us to move a GPS antenna in a known manner with a temporal spectrum similar to a real seismic event. The difference between the antenna position inferred from GPS observations and the known "true" antenna position will yield directly the time-dependent error in the GPS measurements.

## 2. Earthquake Simulator

[5] The simulator (Figure 1) consists of a bidirectional, single-axis positioning table coupled to a digitally controlled stepping motor. Motor speed and direction are controlled by a field programmable gate array (FPGA) chip that synchronously sequences through earthquake profiles stored in erasable programmable read-only memory (EPROM) (see auxiliary material[1] for details). A GPS antenna attached to the positioning table undergoes the simulated seismic motions of the Earth's surface while collecting high-rate GPS data.

[6] We used normal-mode summation [*Gilbert*, 1970] to synthesize 1-Hz, three-dimensional surface displacements for the 3 November 2002, moment magnitude ($M_w$) 7.9 Denali fault earthquake, Alaska [e.g., *Eberhart-Phillips et al.*, 2003], at the location of the Harvard (Mass.) station of the Global Seismographic Network. This station is located at ~5202 km from the epicenter. The duration of the synthesized event was 15 min. The largest ground motions at these teleseismic distances are dominated by surface waves. The synthetic waveforms contained the full spectrum of the ground motions caused by the Denali earthquake up to 0.125 Hz, thus covering the energy band of surface waves. We chose a distant location since the majority of GPS stations for any earthquake will be a long distance from the event, and large (i.e., strong) motions may present issues of GPS signal tracking. We will investigate these larger motions in the future.

[7] The positioning table can be oriented to move along any direction on the horizontal plane. A coupling mechanism also allows the GPS antenna to move along the vertical direction. Since the table displaces in one dimension, we used a single (topocentric) component of the model to drive the simulator at different times. To match approximately the peak-to-peak earthquake displacement to the total travel distance of the positioning table (101.6 mm), we

[1]Harvard-Smithsonian Center for Astrophysics, Cambridge, Massachusetts, USA.
[2]Also at Institute for Space Sciences, CSIC/IEEC, Barcelona, Spain.
[3]Lincoln Laboratory, Massachusetts Institute of Technology, Lexington, Massachusetts, USA.
[4]Institute for Space Sciences, CSIC/IEEC, Barcelona, Spain.
[5]Department of Earth and Planetary Sciences, Harvard University, Cambridge, Massachusetts, USA.


0094-8276/06/2006GL026065$05.00

[1]Auxiliary material is available in the HTML.

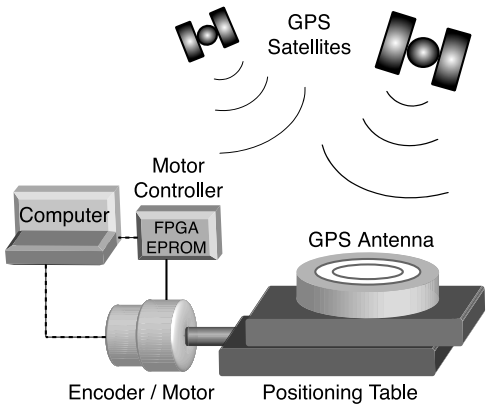


**Figure 1.** Schematic of the GPS earthquake simulator. A laptop computer is used for initialization (controller) and calibration (encoder) purposes only. A GPS antenna is mounted on the positioner table and is displaced according to the simulated earthquake while recording GPS data simultaneously (see auxiliary material[1] for details).

multiplied the predicted deformations of the model by 3.5, thus amplifying the displacement while preserving the spectral characteristics of the simulated event. We then performed a linear interpolation of the 1-Hz model to a rate of 2 kHz to minimize positional errors due to time differences between the epoch of GPS antenna motion and the epoch of the GPS receiver sampling. To assess the accuracy of the simulator, we compared the commanded position of the table (step-size resolution of 6.35 μm) to the position measured by an encoder mounted to the shaft of the stepping motor (measurement uncertainty of 10 μm). The maximum position error over the 15-min duration of the Denali sequence was 0.1 mm, and the root-mean-square (rms) error was 0.05 mm.

## 3. GPS Data Acquisition and Analysis

[8] A GPS antenna (Trimble choke-ring) was attached to the table, and the simulator was operated with the antenna simultaneously feeding two GPS receivers (Ashtech MicroZ-CGRS) that collected data at a sampling rate of 5 Hz. (The second GPS receiver was included for redundancy and calibration purposes, and will not be further discussed here.) We repeated this earthquake sequence every hour for seven hours, with different components of displacement used on different days. Each day was preceded and followed by a "static" day during which the antenna was not moved. A second static GPS antenna located ~10 m from the moving antenna was simultaneously collecting high-rate (5 Hz) GPS data. The same external oscillator was connected to all GPS receivers. Microwave absorber was tucked under both antennas to minimize potential errors due to signal multipath and scattering [e.g., *Elósegui et al.*, 1996].

[9] We used the GIPSY version 2.6 software package [*Lichten and Border*, 1987] and high-precision kinematic data processing methods [e.g., *Elósegui et al.*, 1996; *Larson et al.*, 2001, 2003; *Choi et al.*, 2004] to estimate the position of the moving GPS antenna relative to the static antenna. Although this software will analyze data at rates greater than 1 Hz, it requires special modifications which we have not yet obtained. We have therefore decimated the data for the current study to 1 Hz, which is the highest sampling rate published to date. We restricted the 1-Hz data analysis to a time window of approximately two hours centered on the earthquake simulation. We used JPL precise satellite orbits [*Heflin et al.*, 1992], which were held fixed. The static site served to provide the reference clock. For each epoch, we estimated satellite clock errors, receiver clock errors of the moving site, and the motion of the moving antenna, all modeled as white noise stochastic processes. We also estimated a single position for the static site and a single differential atmospheric zenith delay between the two sites. We used observations above a minimum elevation angle of 15°. The version of GIPSY we used did not allow us to fix carrier phase ambiguities. We do not expect the lack of fixing ambiguities to affect the results of this study [*Larson et al.*, 2002], which concentrates on the north component of site position (see below).

[10] We used modified sidereal filtering [*Choi et al.*, 2004] to calculate a time correction (relative to one sidereal day) to the repeat period of the GPS satellite topocentric positions. The value is determined by calculating rms phase differences between days with a range of offset corrections about zero (corresponding exactly to one sidereal day). The offset value at which the rms difference is minimized is then used in the sidereal filter [*Genrich and Bock*, 1992], which uses phase differences between successive days to remove repeated errors due to, e.g., phase multipath and site and satellite geometry. The minimum offset we found corresponded to a repeat time offset of −10 s, with the minimum being well defined (Figure 2). We assumed that this offset held for all GPS satellites.

## 4. Results

[11] For this initial study, we used a single run that was driven using the north component of displacement. (Full analysis of all components at the full 5-Hz sampling will be presented in a later study.) Figure 3 shows a 15-minute snapshot of the GPS-estimated position time series compared to the true position time series. The maximum modeled displacement amplitude of ~40 mm occurs at a time of ~400 s on this plot. The errors in the GPS determinations (i.e., GPS sidereal filtered position minus known table position) are also shown. Except for a ~14-mm

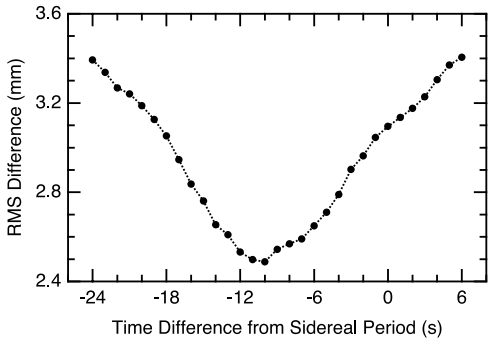


**Figure 2.** RMS difference as a function of the time offset from the sidereal period calculated by differencing the time-dependent position of the moving antenna between two consecutive days. The value of the minimum rms occurs at −10 sec; this offset value is used in the modified sidereal filtering. The sidereal period is 86164 s.

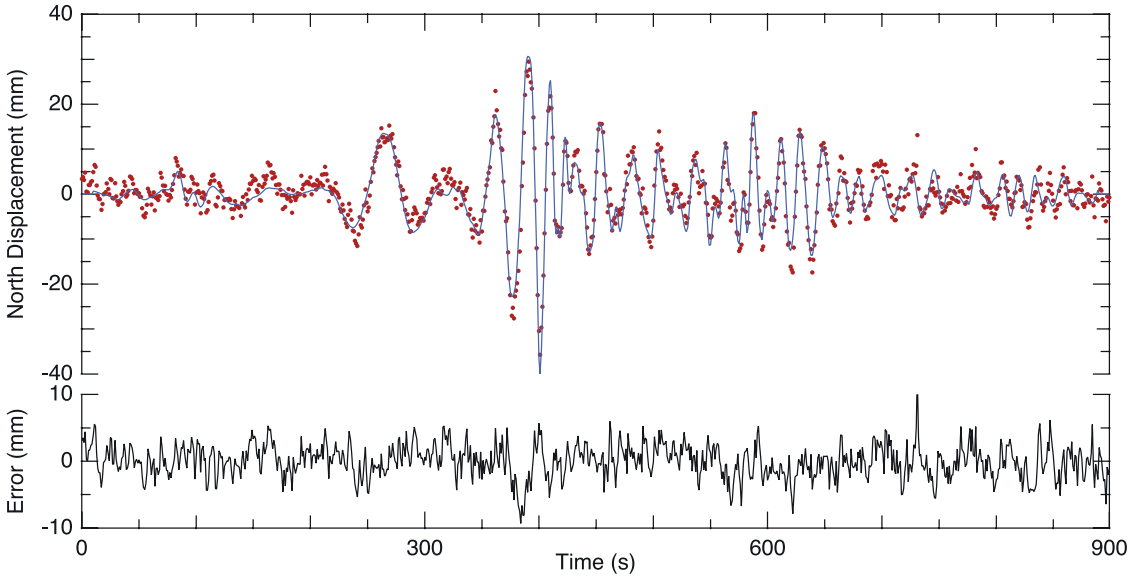


**Figure 3.** Estimates (red dots) of the time-dependent position of the moving platform (blue line) relative to the static antenna for the time of minimum rms error of Figure 2, and their difference (black line).

"glitch" at epoch 731 s (omitted on Figure 3), the amplitude of the maximum error was ~10 mm, and occurred within the period of largest motion. Approximately 96% of the determinations were in error by less than 5 mm. The rms error over the entire event was 2.5 mm.

[12] Based on visual inspection of the upper part of Figure 3, it seems as though the position errors are larger during the period when the antenna motion is smallest. This effect was also noted by *Bock et al.* [2004], who indicated that the GPS errors appear smaller during dynamic periods compared to static periods. As noted above, however, our largest GPS errors were observed during the period of large antenna motions. To test this hypothesis further, we calculated the rms error in 30-sec running-boxcar windows to generate a time series of rms error. In Figure 4 we plot this time series and expand the time window compared to that of Figure 3 to include static periods. During the (now 25-min) timespan, the rms error fluctuates mostly between 2 and 3 mm, exceeding these boundaries on a few occasions. We do not observe a bias in GPS accuracy that is correlated with antenna motion, and we conclude that this may be a visual illusion. Preliminary analysis of three earthquake sequences run one, two, and three hours after this sequence (not shown here) further support this conclusion.

[13] The GPS error clearly has temporal correlations, however. To investigate these, we calculated the power-spectral density (psd, or simply "spectrum") of the GPS error, and compared it to both the psd of the noise in the

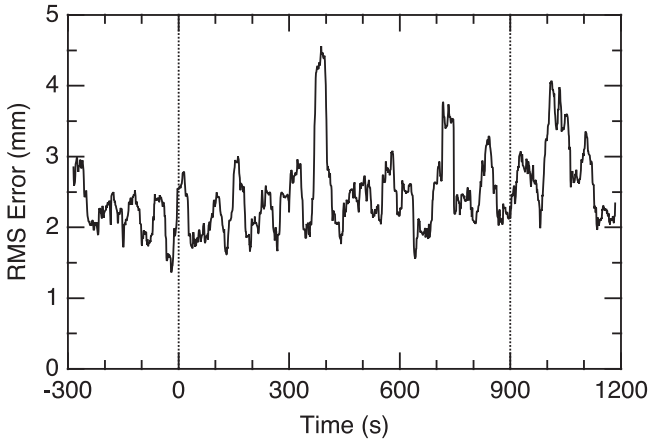


**Figure 4.** RMS error of the time-dependent position estimates of Figure 3 calculated in a 30-s running boxcar. Calculation of rms error has been extended to 300 s immediately before and after the time range of Figure 3 (vertical dotted lines) to include times when the GPS antenna was static.

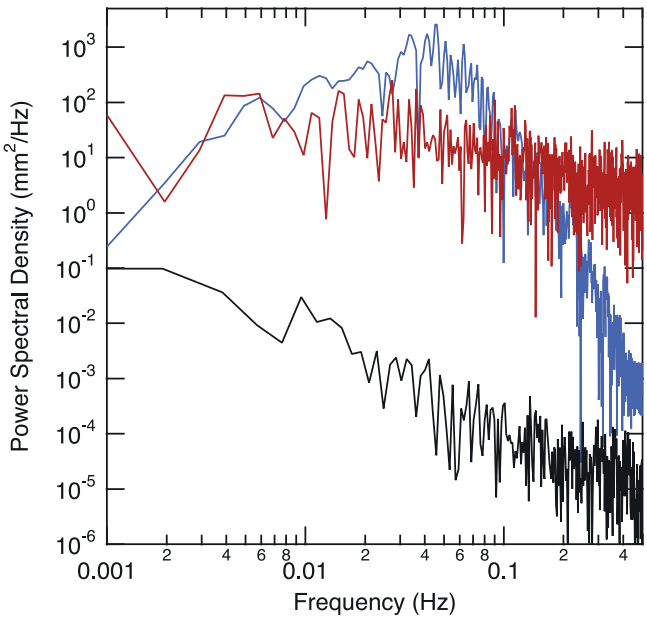


**Figure 5.** Spectra of the time series shown in Figure 3. Color coding consistent with Figure 3.

table position, calculated from the positioner calibration described in Section 2, and a spectral estimate of the original seismic signal, calculated using the same method as for the psd. Figure 5 shows that each of these time series has a different spectrum, qualitatively and quantitatively. The psd of the positioner noise is highly reddened. The spectral index (i.e., the value of $x$ in $S(f) \sim f^x$) is approximately $-2$ at the lower frequencies, indicating a random-walk process. This result is understandable, given the method by which the positioner was driven (Section 2). Values of the psd of the positioner noise are generally 2–5 orders of magnitude smaller than the psd of the error. This result verifies that we can ignore the positioning error of the earthquake simulator, and that for practical purposes this simulator is "ground truth."

[14] The spectrum of the GPS error is also reddened, but not as steeply as the positioner noise psd. The spectral index of the GPS error is approximately $-1$, indicating flicker noise. This behavior is common for complex systems, and represents the combined effect of noise in GPS receiver electronics as well as errors in models describing the receiver and antenna phase variations, satellite orbit positions, atmosphere (neutral and charged), approximations made in data analysis, and many other small errors. We also calculated the autocorrelation function (the Fourier transform of the psd) of the GPS error, which yields a decorrelation time for the position error of 1.55 s. Position estimates separated by less than this time will be correlated by more than 50%.

[15] The spectrum of the synthetic seismogram is more complex than either of the other two curves. Its characteristics represent the particular seismic process being modeled (see Section 2), and will be different depending on the type of event and the distance from the source. For the event used in this study, the spectral estimate of the synthetic seismic displacement signal exceeds the GPS noise spectrum within a band bounded by $\sim$0.01 and $\sim$0.1 Hz. At frequencies above (by construction) and below this band, the spectrum of the synthetic seismic signal drops off more rapidly than the spectrum of the GPS error. These results indicate that there may be a maximum GPS data acquisition rate above which the GPS data yield no useful information, at least for teleseismic events, which are dominated by surface waves.

[16] Our results are important for designing and planning experiments using GPS and other GNSS such as Glonass and Galileo. Increasing the data acquisition rate significantly increases the burden on data storage, transmission, and archiving, thereby translating into greater expense. To some extent, our results represent a best-case scenario, since we eliminated or reduced some forms of error that generally exist under normal conditions. For example, we reduced multipath errors through the use of microwave absorber, and eliminated station clock errors and reduced atmospheric errors by differencing with a close reference station driven by the same frequency standard. In addition, our antenna was moving thus slightly changing its multipath environment. Further investigations will attempt to isolate the effect of each of these errors on the high-rate GPS technique.

[17] **Acknowledgments.** We would like to express our gratitude to R. Blundell, R. Kimberk, and S. Leiker of SAO Receiver Lab for assistance constructing and calibrating the translation table. We thank A. Petit and C. Moreno of Begues City Hall, J. Normandeau of UNAVCO, Inc., and O. Nogues, A. Rius, and J. Torrobella of IEEC for assistance with the GPS experiment. We thank two anonymous reviewers for helpful comments. Some equipment was loaned from the UNAVCO Facility. This research was funded by NASA grant NAG5-13748 and Spanish Ministry of Education and Science grants ESP2004-00218 and CGL2004-21479-E.

## References

Bock, Y., L. Prawirodirdjo, and T. I. Melbourne (2004), Detection of arbitrarily large ground motions with a dense high-rate GPS network, *Geophys. Res. Lett.*, *31*, L06604, doi:10.1029/2003GL019150.

Choi, K., A. Bilich, K. M. Larson, and P. Axelrad (2004), Modified sidereal filtering: Implications for high-rate GPS positioning, *Geophys. Res. Lett.*, *31*, L22608, doi:10.1029/2004GL021621.

Eberhart-Phillips, D., et al. (2003), The 2002 Denali fault earthquake: A large magnitude, slip-partitioned event, *Science*, *300*, 1113–1118.

Elósegui, P., J. L. Davis, J. M. Johansson, and I. I. Shapiro (1996), Detection of transient motions with the Global Positioning System, *J. Geophys. Res.*, *101*, 11,249–11,261.

Genrich, J. F., and Y. Bock (1992), Rapid resolution of crustal motion at short ranges with the global positioning system, *J. Geophys. Res.*, *97*, 3261–3269.

Gilbert, F. (1970), Excitation of the normal modes of the Earth by earthquake sources, *Geophys. J. R. Astron. Soc.*, *22*, 223–226.

Heflin, M., et al. (1992), Global geodesy using GPS without fiducial sites, *Geophys. Res. Lett.*, *19*, 131–134.

Ji, C., K. M. Larson, Y. Tan, K. W. Hudnut, and K. Choi (2004), Slip history of the 2003 San Simeon earthquake constrained by combining 1-Hz GPS, strong motion, and teleseismic data, *Geophys. Res. Lett.*, *31*, L17608, doi:10.1029/2004GL020448.

Kato, T., Y. Terada, K. Ito, R. Hattori, T. Abe, T. Miyake, S. Koshimura, and T. Nagai (2005), Tsunami due to the 2004 September 5th off the Kii Peninsula earthquake, Japan, recorded by a new GPS buoy, *Earth Planets Space*, *57*, 297–301.

Larson, K. M., P. Cervelli, M. Lisowski, A. Miklius, P. Segall, and S. Owen (2001), Volcano monitoring using the Global Positioning System: Filtering strategies, *J. Geophys. Res.*, *106*, 19,453–19,464.

Larson, K., J. Plumb, J. Zwally, and W. Abdalati (2002), Analysis of GPS data collected on the Greenland ice sheet, *Polar Geogr.*, *25*, 22–40.

Larson, K. M., P. Boden, and J. Gomberg (2003), Using 1-Hz GPS data to measure deformations caused by the Denali fault earthquake, *Science*, *300*, 1421–1424.

Lichten, S. M., and J. S. Border (1987), Strategies for high-precision Global Positioning System orbit determination, *J. Geophys. Res.*, *92*, 12,751–12,762.

Mattia, M., M. Rossi, F. Guglielmino, M. Aloisi, and Y. Bock (2004), The shallow plumbing system of Stromboli Island as imaged from 1 Hz instantaneous GPS positions, *Geophys. Res. Lett.*, *31*, L24610, doi:10.1029/2004GL021281.

Miyazaki, S., K. M. Larson, K. Choi, K. Hikima, K. Koketsu, P. Bodin, J. Haase, G. Emore, and A. Yamagiwa (2004), Modeling the rupture process of the 2003 September 25 Tokachi-Oki (Hokkaido) earthquake using 1-Hz GPS data, *Geophys. Res. Lett.*, *31*, L21603, doi:10.1029/2004GL021457.

R. Baena, Institute for Space Sciences, CSIC/IEEC, Gran Capitan 2, E-08034 Barcelona, Spain. (rbaena@ieec.fcr.es)

J. L. Davis and P. Elósegui, Harvard-Smithsonian Center for Astrophysics, 60 Garden Street (MS-42), Cambridge, MA 02138, USA. (jdavis@cfa.harvard.edu; pelosegui@cfa.harvard.edu)

G. Ekström, Department of Earth and Planetary Sciences, Harvard University, 20 Oxford Street, Cambridge, MA 02138, USA. (ekstrom@eps.harvard.edu)

D. Oberlander, Lincoln Laboratory, Massachusetts Institute of Technology, 244 Wood Street, Lexington, MA 02420, USA. (oberlander@ll.mit.edu)